Available online at www.sciencedirect.com

ScienceDirect

Ceramics International 39 (2013) 9415–9419

CERAMICS INTERNATIONAL

www.elsevier.com/locate/ceramint

Transparent sub-micrometre alumina from lanthanum oxide doped common grade alumina powder

P. Biswas, M. Kiran Kumar, K. Rajeswari, R. Johnson, U.S. Hareesh*

Centre for Ceramic Processing, International Advanced Research Centre for Powder Metallurgy and New Materials, Balapur PO, Hyderabad 500005, India

Received 15 April 2013; received in revised form 10 May 2013; accepted 11 May 2013
Available online 23 May 2013

Abstract

Common grade high purity alumina (99.99%) powder doped with lanthanum oxide was slip cast, dried and pressureless sintered to sub-micrometre grain sized alumina at 1380–1410 °C. Samples that attained $>96\%$ theoretical density (TD) were subsequently hot isostatically pressed to fully dense alumina having $\geq 99.95\%$ TD. Sintered sub-micrometre alumina samples, ground to 2 mm thickness and polished to 0.5 μm surface finish, displayed $>82\%$ transmission in the 3–5 μm wavelength range. Samples of 0.5 mm thickness also exhibited 40–60% transmission in the visible wavelength region of 400–900 nm. Lanthanum oxide addition within 0.10 wt% was shown to be favourable for improved transparency in the visible region. The alumina samples also exhibited high Vickers hardness values of 2144+45 kg/mm^2 at 5 kg indentation load.

Keywords: A. Hot isostatic pressing; A. Slip casting; C. Hardness; D. Al_2O_3; E. Lamp envelopes

1. Introduction

Polycrystalline alumina (PCA), when densified to $\geq 99.95\%$ density with sub-micrometre grain sizes, has been shown to be transparent to electromagnetic radiations in the spectral regions of 3–5 μm (infrared) and 400–900 nm (visible) wavelengths [1–15]. Although single crystal aluminium oxide, commonly known as sapphire, is also transparent in the above spectral regions, the crystal growth of sapphire and the associated post-machining costs are enormous and its mechanical properties are inferior to that of polycrystalline alumina. PCA with sub-micrometre grain sizes, near theoretical density ($\geq 99.95\%$ TD) and enhanced mechanical properties of strength and hardness has been successfully developed by colloidal processing techniques. Krell et al. conceptualised and implemented the development of sintered sub-micrometre alumina and utilised it for a variety of applications ranging from transparent armour to high pressure lamp envelopes [1–9]. Colloidal forming, gel and slip casting, were employed for fabrication of samples with different shapes and hot isostatic pressing (HIP) was engaged for near full densification of samples. High purity, high cost alumina powders (>115 $/kg, TM-DAR, Taimei Corporation, Japan) were used in all the developments. Alternatively, spark plasma sintering (SPS) by virtue of its rapid heating rates and very short soaking times was employed to develop alumina with sintered grain sizes of less than 1 μm [11–16]. However, the SPS technique is limited to samples of flat geometry. Two stage sintering, exploiting a kinetic window, has also been demonstrated as a suitable sintering technique to develop sintered sub-micrometre alumina [17]. This technique also suffers from the drawback of extended soaking times, though at lower temperatures of ~1200 °C, for achieving the density levels required for HIPing.

Efforts have also been made in powder processing to attain highly dense alumina with submicrometre grain sizes. Messing et al. employed sinter forging of sol–gel derived γ-alumina aggregates, seeded with α-alumina, to obtain sub-micrometre grained transparent alumina [18]. The consolidation method of float packing followed by sintering was also employed for the

*Corresponding author. Present address: Materials Science and Technology Division, National Institute for Interdisciplinary Science and Technology (NIIST), Council of Scientific and Industrial Research (CSIR), Industrial Estate PO, Thiruvananthapuram 695019, India. Tel.: +91 4712535504; fax: +91 4712491712.

E-mail addresses: hareesh@niist.res.in, ushareeshnair@gmail.com (U.S. Hareesh).

0272-8842/$ - see front matter © 2013 Elsevier Ltd and Techna Group S.r.l. All rights reserved.
http://dx.doi.org/10.1016/j.ceramint.2013.05.058

development of transparent alumina [19]. Surface modification by hydrofluoric acid treatment of aggregated alumina powders was shown to be an effective technique for the development of transparent alumina by spark plasma sintering [13]. On compositional modifications, the effect of dopants on densification and grain growth kinetics of alumina has been widely reported in the literature for micron sized alumina and spark plasma sintered sub-micrometre alumina [20–27]. However, systematic experimental investigations on the role of La_2O_3 on infrared and visible transparency of sintered sub-micrometre PCA, by post sintering HIPing, has not been attempted though it was successfully employed in a US patent, US-2007/0278960 A1 [28]. The present study therefore explores a defect free colloidal processing of common grade, low cost (~30 $/kg) high purity alumina powders for the development of transparent PCA.

2. Experimental methods

Commercially available high purity alumina powder (99.99%, Ceralox AHPA 0.5, Sasol North America Inc., Tucson, AZ, doped with 500 ppm MgO) was dispersed in aqueous medium to obtain slurries of 76 wt% solid loading. In a typical experimental batch, 76 g of alumina powder was dispersed in 24 g water under constant stirring. pH of suspension was maintained at 4 by intermittent addition of nitric acid (Qualigens, India, 10 wt%). The alumina suspension was then mixed with 0, 0.10, 0.25, 0.5 and 1 wt% La_2O_3 powders (Sigma Aldrich, USA) and ball milled for 12 h in polypropylene bottles with a pot jar mill. Alumina balls of 2 mm diameter, at a 1:1 charge to balls ratio, were used as the milling medium. Octanol was used as an antifoaming agent. Rheological characterisation (MCR 51, Anton Paar, Austria) of the slurries was then carried out at 25 °C using a parallel plate configuration, varying the shear rates from 13 to 1000 s^{-1}. Slurries after deairing were cast into shapes of 15 mm × 15 mm square blanks on a porous alumina plate of 5 mm thickness and dried further at 45 °C and 75% RH for 24 h in a controlled humidity chamber (Remi Instruments, Mumbai, India). Pressureless sintering was then performed in air (Nabertherm, Bremen, Germany) over 1325–1410 °C. Density of the samples was measured by using the Archimedes method. Samples having > 96% theoretical density were subjected to hot isostatic pressing (HIP, American Isostatic Press, USA) at 1350 °C for 5 h under argon atmosphere. HIPed samples were ground to varying thicknesses and polished to 0.5 μm surface finish. Transmission patterns of the samples in the wavelength region of 2–5 μm was measured by using Fourier Transform Spectrophotometer (FTIR, Spectrum-GX, Perkin Elmer, Singapore) and in the visible region of 400–900 nm by using a visible spectrophotometer (UV–visible, Perkin Elmer, Singapore). Microstructural examinations of polished and thermally etched (1300 °C/30 min) samples were carried out by using scanning electron microscopy (Hitachi 3200 S, FE-SEM, Tokyo, Japan). Hardness evaluation of the samples was performed by Vickers indentation (Leco, St. Joseph, MI) at 5 kg loads.

3. Results and discussion

Viscosity, at varying shear rates, of the alumina slurries containing different amounts of La_2O_3 are presented in Fig. 1. The 76 wt% alumina slurry without La_2O_3 possessed viscosity values of less than 1 Pa s and followed a reducing trend with increasing shear rates, suggesting shear thinning behaviour. This is quite conducive for colloidal forming processes as it prevents the alumina particles from settling during casting. Further addition of La_2O_3 up to 0.25 wt% showed negligible effect on the rheological behaviour of alumina slurry and the viscosity curves almost overlap each other. However, as the La_2O_3 content exceeded beyond 0.25 wt%, the viscosity values increased to almost double as that of the slurry without La_2O_3.

Fig. 2 shows relative densities of the alumina samples, as a function of contents of La_2O_3, sintered at 1320, 1350, 1380 and 1420 °C. At all sintering temperatures La_2O_3 was found to impede densification and the effect is much prominent at lower sintering temperatures (1320 and 1350 °C).

Density of > 96% TD is achieved only at the sintering temperatures of 1380 and 1410 °C for samples with up to 0.5 wt% La_2O_3. It has been reported that the large ionic radius mismatch between Al^{3+} and La^{3+} (1.06 Å for La^{3+} and 0.51 Å for Al^{3+}) forced La^{3+} ions to segregate at the grain boundaries

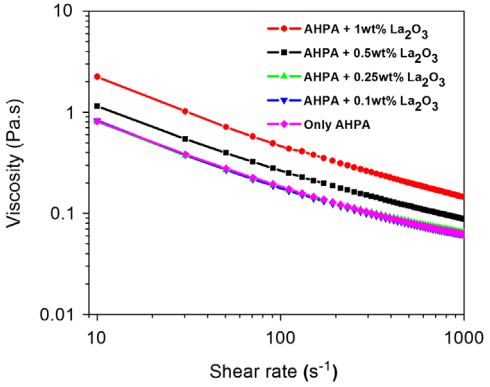

Fig. 1. Viscosity with shear rates for alumina slurries with varying La_2O_3 contents.

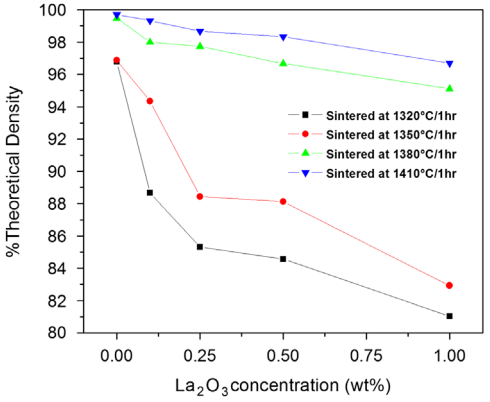

Fig. 2. Relative densities of the alumina samples as a function of the amounts of La_2O_3 sintered at different temperatures.

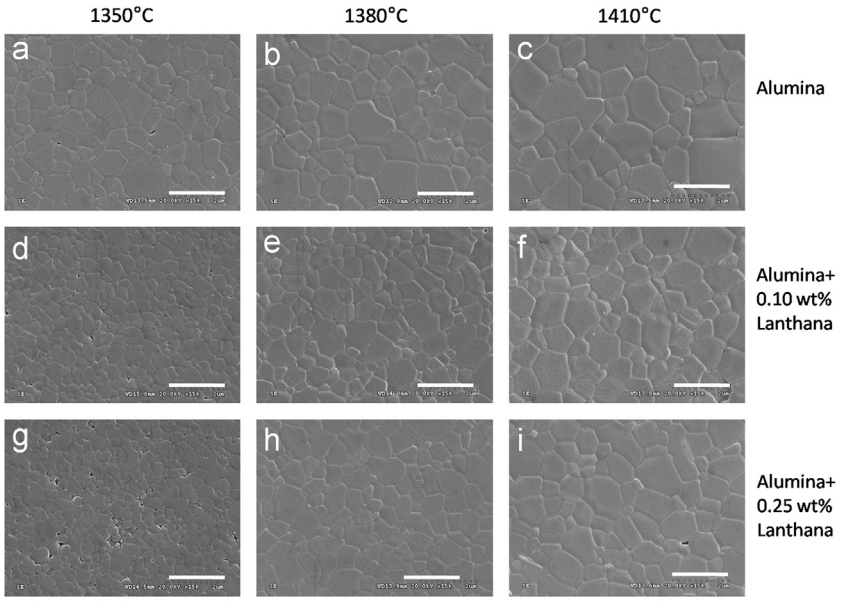

Fig. 3. SEM images of the polished and thermally etched alumina samples without La_2O_3 (a—1350 °C, b—1380 °C and c—1410 °C), with 0.10 wt% La_2O_3 (d—1350 °C, e—1380 °C and f—1410 °C) and with 0.25 wt% La_2O_3 (g—1350 °C, h—1380 °C and i—1410 °C) [magnification bar is 2 μm].

as second phases in order to reduce the elastic strain energy arising from the ionic radii mismatch [21,22,25,26]. Also, La cations tended to block the diffusion of ions along grain boundaries, leading to reduced grain boundary diffusivity and hence decreased densification rate [26]. The densification rate of ultrahigh purity alumina doped with 1000 ppm lanthanum is reduced by a factor of 21.

SEM images of the polished and thermally etched specimens, with and without La_2O_3, pressureless sintered in the temperature range of 1350–1410 °C, are presented in Fig. 3. The microstructural observations complimented the densification data and it is clearly observed that La_2O_3 addition is an impediment to densification, particularly at the lower sintering temperatures of 1350 and 1380 °C. The microstructures of the 1380 and 1410 °C samples are characteristic of dense alumina while the 1350 °C one has few scattered pores. The average grain size increased from 0.90 μm to >1.5 μm as the sintering temperature is increased from 1350–1380 °C to 1410 °C. Fig. 3(d–f) depicts microstructural features of the alumina samples containing 0.10 wt% La_2O_3.

There is significant reduction in alumina grain sizes on La_2O_3 addition and the resultant microstructure is uniform with fine grains in the samples sintered at 1350–1410 °C. Isolated pores are observed in the 1350 °C sample (Fig. 3(d)) while the high temperature ones (Fig. 3(e) and (f)) are fully dense. As the La_2O_3 content is increased to 0.25 wt%, the sample sintered at 1350 °C is relatively porous (Fig. 3(g)). The reduction in grain size on La_2O_3 addition is further confirmed in these samples. Denser samples are obtained on increase of temperature to 1380 and 1410 °C.

Grain sizes of the alumina samples, containing 0, 0.1 and 0.25 wt% La_2O_3, sintered at 1350–1410 °C are presented in Fig. 4. The average grain sizes of the doped samples are lower

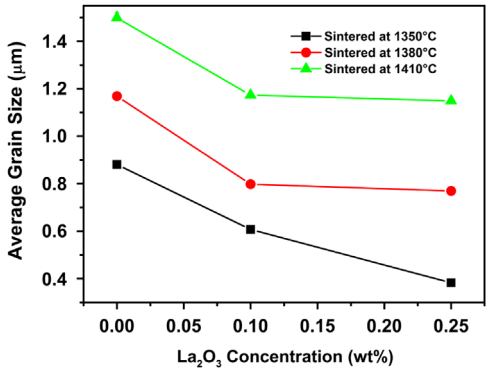

Fig. 4. Average grain sizes of the alumina with various concentrations of La_2O_3 and pressureless sintered at 1350, 1380 and 1410 °C.

than that of the undoped ones at 1350, 1380 and 1410 °C. The microstructural examinations clearly indicated a beneficial effect of La_2O_3 addition on controlling grain growth of the samples during sintering.

Fig. 5 presents the SEM images of the alumina samples containing 0.5 and 1.0 wt% La_2O_3 sintered at 1410 °C. Intergranular pores are scattered in the samples and these samples had relatively lower density as compared to that with lower concentrations of La_2O_3. Based on this observation, samples containing up to 0.25 wt% La_2O_3 sintered at 1380–1410 °C with density of $>96\%$ TD were subjected to hot isostatic pressing at 1350 °C for 5 h. Near full densification (99.95% TD) was obtained for all samples that fulfilled the above criterion. Microstructural analysis (Fig. 6) showed that there was no further grain growth and average grain size of the sintered and HIPed samples were in the range of 0.6–0.8 μm.

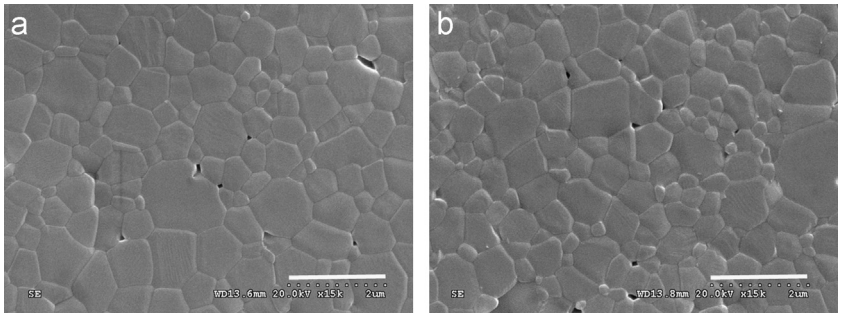

Fig. 5. SEM images of the polished and thermally etched alumina samples (a) with 0.50 wt% La_2O_3 at1410 °C and (b) with 1.0 wt% La_2O_3 at 1410 °C [magnification bar is 2 μm].

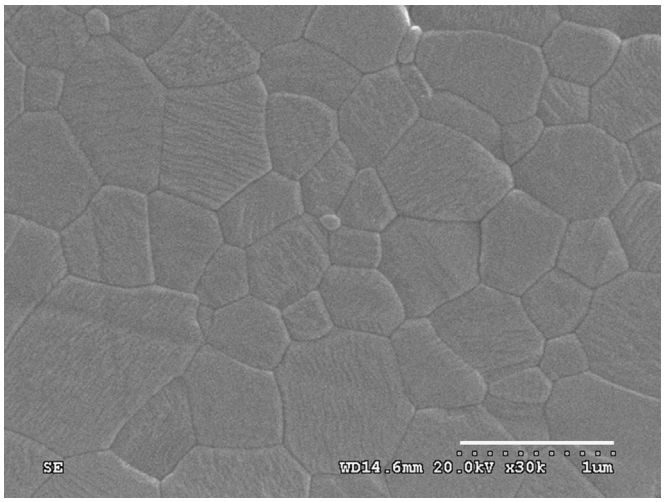

Fig. 6. SEM image of the polished and thermally etched alumina sample with 0.10 wt% La_2O_3 sintered at 1380 °C and hot isostatically pressed at 1350 °C/ 5 h [magnification bar is 1 μm].

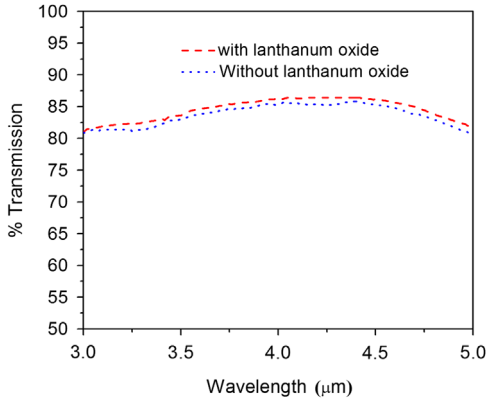

Fig. 7. IR transmission pattern of the alumina samples with and without La_2O_3.

Transmission behaviour of the alumina samples with and without La_2O_3 over 3–5 μm is presented in Fig. 7. Measurements were carried out on samples with 2 mm thickness and 0.5 μm surface finish. There is a slight difference between the two samples. The transmission values are very close to the theoretical value of 86% reported for sapphire.

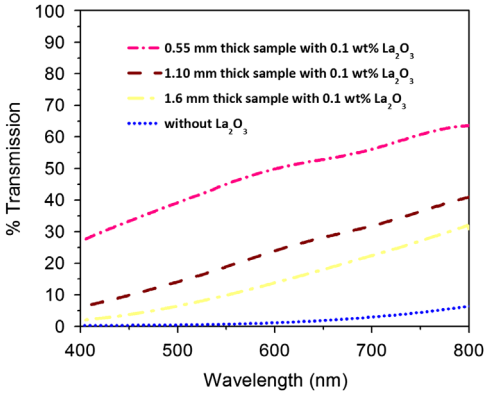

Fig. 8. Transmission patterns of the alumina samples with and without La_2O_3 in the wavelength region of 400–800 nm.

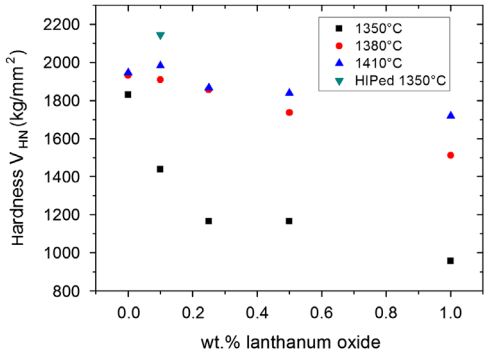

Fig. 9. Indentation hardness values of the pressure less sintered alumina samples with different concentrations of La_2O_3, compared with that of the HIPed sample containing 0.1 wt% La_2O_3.

Fig. 8 presents transmission patterns in the visible region of 400–900 nm. The alumina sample with 1 mm thickness and without La_2O_3 exhibited nearly zero transmission while those with 0.10 wt% La_2O_3 showed improved transparency with a strong dependency on thickness. The samples displayed a trend of increasing transmission with increasing wavelength.

Fig. 9 denotes Vickers indentation hardness of the pressureless sintered alumina samples containing varying concentrations of La_2O_3. Complimentary to the densification data,

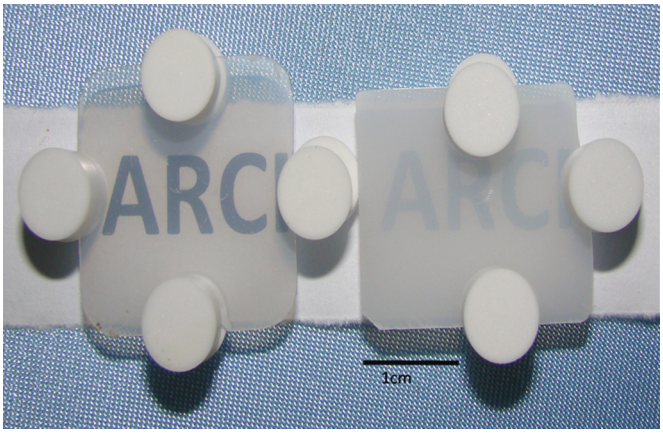

Fig. 10. Photograph demonstrating visible transparency of the alumina sample containing 0.1 wt% La_2O_3 (sample is 8 mm above the print ARCI).

hardness values indicated a decreasing trend with increasing La_2O_3 content for the same sintering temperature. Samples sintered at 1380 and 1410 °C displayed similar values for the La_2O_3 contents of 0, 0.1 and 0.25 wt%. HIPed alumina sample containing 0.1 wt% La_2O_3 yielded a value of 2144+45 kg/mm^2 (for 10 measurements) under the indentation load of 5 kg.

Fig. 10 displays photographs of the alumina samples, with 0 and 0.1 wt% La_2O_3 HIPed at 1350 °C. The beneficial effect of La_2O_3 addition on visible transparency is well demonstrated for the sample that is kept 8 mm above the printed matter (where the letters ARCI is clear and legible) in comparison to that of the undoped one which has negligible visible transparency.

4. Conclusion

The present study has demonstrated the suitability of a common grade alumina powder for the development of transparent alumina with submicrometre sintered grain sizes. La_2O_3 addition within 0.25 wt% could be used to control the grain growth behaviour and the microstructural refinement of alumina ceramics with improved IR and visible transparency.

References

[1] A. Krell, P. Blank, H.W. Ma, T. Hutzler, M.P.B. van Bruggen, R. Apetz, Transparent sintered corundum with high hardness and strength, Journal of the American Ceramic Society 86 (1) (2003) 12–18.
[2] A. Krell, H.W. Ma, Nanocorundum—advanced synthesis and processing, Nanostructured Materials 11 (8) (1999) 1141–1153.
[3] A. Krell, H.W. Ma, Sintering transparent and other sub-micrometer alumina: the right powder, Ceramic Forum International 80 (4) (2003) E41–E45.
[4] A. Krell, J. Klimke, T. Hutzler, Advanced spinel and sub-μm Al_2O_3 for transparent armour applications, Journal of the European Ceramic Society 29 (2009) 275–281.
[5] A. Krell, T. Hutzler, J. Klimke, Transmission physics and consequences for materials selection, manufacturing, and applications, Journal of the European Ceramic Society 29 (2009) 207–221.
[6] A. Krell, J. Klimke, T. Hutzler, Transparent compact ceramics: inherent physical issues, Optical Materials 31 (8) (2009) 1144–1150.
[7] A. Krell, G. Baur, C. Dahne, Transparent sintered sub-micrometre Al_2O_3 with IR transmissivity equal to sapphire, in: R.W. Tustison (Ed.), Proceedings of the Society of Photo-Optical Instrumentation Engineers (SPIE), Window and Dome Technologies VIII, vol. 5078, 2003, pp. 199–207.
[8] A. Krell, P. Blank, H.W. Ma, T. Hutzler, M. Nebelung, Processing of high-density submicrometer Al_2O_3 for new applications, Journal of the American Ceramic Society 86 (4) (2003) 546–553.
[9] A. Krell, S. Schadlich, Nanoindentation hardness of submicrometer alumina ceramics, Materials Science and Engineering A 307 (1–2) (2001) 72–81.
[10] R. Apetz, M.P.B. van Bruggen, Transparent alumina: a light-scattering model, Journal of the American Ceramic Society 86 (3) (2003) 480–486.
[11] B.N. Kim, K. Hiraga, K. Morita, H. Yoshida, Spark plasma sintering of transparent alumina, Scripta Materialia 57 (7) (2007) 607–610.
[12] B.N. Kim, K. Hiraga, K. Morita, H. Yoshida, T. Miyazaki, Y. Kagawa, Microstructure and optical properties of transparent alumina, Acta Materialia 57 (2009) 1319–1326.
[13] X.H. Jin, L. Gao, J. Sun, Highly transparent alumina spark plasma sintered from common-grade commercial powder: the effect of powder treatment, Journal of the American Ceramic Society 93 (5) (2010) 1232–1236.
[14] D. Chakravarty, G. Sundararajan, Effect of applied stress on IR transmission of spark plasma-sintered alumina, Journal of the American Ceramic Society 93 (4) (2010) 951–995.
[15] M. Stuer, Z. Zhao, U. Aschauer, P. Bowen, Transparent polycrystalline alumina using spark plasma sintering: effect of Mg, Y and La doping, Journal of the European Ceramic Society 30 (6) (2010) 1335–1343.
[16] N. Roussel, L. Lallemant, B. Durand, S. Guillemet, J.-Y.C. Ching, G. Fantozzi, V. Garnier, G. Bonnefont, Effects of the nature of the doping salt and of the thermal pre-treatment and sintering temperature on spark plasma sintering of transparent alumina, Ceramics International 37 (2011) 3565–3573.
[17] K. Bodisova, P. Sajgalik, D. Galusek, P. Svancarek, Two-stage sintering of alumina with submicrometer grain size, Journal of the American Ceramic Society 90 (1) (2007) 330–332.
[18] O.H. Kwon, C.S. Nordahl, G.L. Messing, Submicrometer transparent alumina by sinter forging seeded gamma-Al_2O_3 powders, Journal of the American Ceramic Society 78 (2) (1995) 491–494.
[19] D. Godlinski, M. Kuntz, G. Grathwohl, Transparent alumina with submicrometer grains by float packing and sintering, Journal of the American Ceramic Society 85 (10) (2002) 2449–2456.
[20] J. Cho, C.M. Wang, H.M. Chan, J.M. Rickman, M.P. Harmer, A study of grain-boundary structure in rare-earth doped aluminas using an EBSD technique, Journal of Materials Science 37 (1) (2002) 59–64.
[21] S. Galmarini, U. Aschauer, A. Tewari, Y. Aman, C. Van Gestel, P. Bowen, Atomistic modeling of dopant segregation in alpha-alumina ceramics: coverage dependent energy of segregation and nominal dopant solubility, Journal of the European Ceramic Society 31 (15) (2011) 2839–2852.
[22] J.H. Cho, M.P. Harmer, H.M. Chan, J.M. Rickman, A.M. Thompson, Effect of yttrium and lanthanum on the tensile creep behavior of aluminum oxide, Journal of the American Ceramic Society 80 (4) (1997) 1013–1017.
[23] E. Sato, C. Carry, Yttria doping and sintering of submicrometer-grained alpha-alumina, Journal of the American Ceramic Society 79 (8) (1996) 2156–2160.
[24] J. Bruley, J. Cho, H.M. Chan, M.P. Harmer, J.M. Rickman, Scanning transmission electron microscopy analysis of grain boundaries in creep-resistant yttrium- and lanthanum-doped alumina microstructures, Journal of the American Ceramic Society 82 (10) (1999) 2865–2870.
[25] C.M. Wang, H.M. Chan, M.P. Harmer, Effect of Nd_2O_3 doping on the densification and abnormal grain growth behavior of high-purity alumina, Journal of the American Ceramic Society 87 (3) (2004) 378–383.
[26] J.X. Fang, A.M. Thompson, M.P. Harmer, H.M. Chan, Effect of yttrium and lanthanum on the final-stage sintering behavior of ultrahigh-purity alumina, Journal of the American Ceramic Society 80 (1997) 2005–2012.
[27] H. Wang, H. Lin, W. Li, J. Shi, Effect of La doping on microwave dielectric properties of translucent polycrystalline alumina ceramic, Ceramics International 39 (2013) 4907–4911.
[28] M.P.B. van Bruggen, T.A. Kop, T.A.P.M. Keursten, US Patent US2007/0278960, 2007.